

7-1-2021

An Early Triassic Small Shelly Fossil-Style Assemblage from the Virgin Limestone Member, Moenkopi Formation, Western United States

Vivienne Maxwell
Smith College

Ben Thuy
Natural History Museum Luxembourg

Sara B. Pruss
Smith College, spruss@smith.edu

Follow this and additional works at: https://scholarworks.smith.edu/geo_facpubs



Part of the [Geology Commons](#)

Recommended Citation

Maxwell, Vivienne; Thuy, Ben; and Pruss, Sara B., "An Early Triassic Small Shelly Fossil-Style Assemblage from the Virgin Limestone Member, Moenkopi Formation, Western United States" (2021). Geosciences: Faculty Publications, Smith College, Northampton, MA.
https://scholarworks.smith.edu/geo_facpubs/172

This Article has been accepted for inclusion in Geosciences: Faculty Publications by an authorized administrator of Smith ScholarWorks. For more information, please contact scholarworks@smith.edu



An Early Triassic small shelly fossil-style assemblage from the Virgin Limestone Member, Moenkopi Formation, western United States

VIVIENNE MAXWELL, BEN THUY  AND SARA B. PRUSS 

LETHAIA



Maxwell, V., Thuy, B., & Pruss, S. B. 2021: An Early Triassic small shelly fossil-style assemblage from the Virgin Limestone Member, Moenkopi Formation, western United States. *Lethaia*, Vol. 54, pp. 368–377.

Small shelly fossils (SSFs) are minute fossils moulded or replaced by apatite, and less commonly, other minerals like glauconite and iron oxides. This taphonomic mode is best known from Cambrian deposits, though some occurrences occur across geological time. Instances of small shelly-style preservation were found in insoluble residues from the Lower Triassic Virgin Limestone Member exposed in southern Nevada, the western United States, a second such occurrence known from this unit. Fossil steinkerns of tiny brachiopods, echinoid spines and ophiuroids are fluorapatite, with scarce phosphatic internal moulds of bivalves and two replaced ostracods. In contrast, the crinoid ossicles, almost all of which are >1000 µm, are preserved as stereomic moulds of silica or dolomite. Though the style of preservation is similar to another Virgin Limestone small shelly fossils-style assemblage, this assemblage preserves greater diversity, likely reflecting the variation in palaeocommunities across the shelf. The size selectivity of phosphatization is clear, as the majority of the fossils <1000 µm are phosphatized. Importantly, the original skeletal material does not exert the strongest control on style of preservation: crinoid ossicles are replaced or moulded by silica whilst ophiuroid and echinoid fragments are phosphatized. It is likely that the underlying phosphatization mechanisms are related to the small particle size of the skeletons or skeletal elements coupled with the local pore water environment. Early Triassic equatorial seas characterized by warm temperatures and lower oxygen levels likely fostered small shelly fossil-style preservation across the shelf during this time. □ *Apatite, Lower Triassic, mass extinction, steinkern, taphonomy.*

Vivienne Maxwell [vmaxwell@smith.edu], Department of Geosciences, Smith College, Northampton, MA 01063, USA; Ben Thuy [ben.thuy@mnhn.lu], Department of Palaeontology, Natural History Museum Luxembourg, Luxembourg City, Luxembourg; Sara B. Pruss  [spruss@smith.edu], Department of Geosciences, Smith College, Northampton, MA 01063, USA; manuscript received on 16/07/2020; manuscript accepted on 26/09/2020.

Small shelly fossil-style preservation is a unique taphonomic mode in which minute fossils are moulded or replaced by apatite, glauconite and other minerals (e.g. Brasier 1990; Porter 2004; Creveling *et al.* 2014a, 2014b), often resulting in ‘microsteinkerns’ (e.g. Datilo *et al.* 2019). This particular style of fossilization is best known from Cambrian deposits, where small shelly fossils record remnants of some early biomineralizers of the Cambrian Explosion and occur across clades. Whilst scattered occurrences of small shelly-style fossilization have been reported from other time periods (Dzik 1994; Datilo *et al.* 2019; Freeman *et al.* 2019), the best known and most intensively studied occurrences are Cambrian small shelly fossils (SSFs), in part because the diversity of organisms preserved in this way is not well represented in macrofossil assemblages. The prevalence of Cambrian SSFs, and their apparent decline in the Paleozoic and post-Paleozoic, has been the subject of work seeking to explain the closing of

this taphonomic window (Porter 2004; Creveling *et al.* 2014a, 2014b), though recent work has questioned the notion that a taphonomic window existed (Datillo *et al.* 2019; Freeman *et al.* 2019).

Previous work that focused explicitly on the recorded occurrences of SSFs in the Cambrian itself showed that, from the early to the middle Cambrian, the abundance of small shelly fossil occurrences declined (Porter 2004). The spike and decline, therefore, might be linked to Fe and P cycling under low-oxygen conditions which led to phosphatization of skeletons (Creveling *et al.* 2014b). Cambrian small shelly fossils occur in a range of settings, so are there generalities that can be made about all small shelly fossil-style preservation, or are there a set of rules that may foster this style of preservation across geological time? Some post-Cambrian examples of small shelly fossil-style preservation may be linked to sedimentary hiatuses and changes in sedimentary regime allowing for the concentration of phosphate and

phosphatic fossils (Freeman *et al.* 2019), but this does not explain all post-Cambrian occurrences (e.g. Pruss *et al.* 2018), and may not explain many of them within the Cambrian.

More recently, SSF-style preservation has been documented from Lower Triassic limestones of the Virgin Limestone Member in shallow water settings exposed in the Muddy Mountains of southeastern Nevada. This work revealed minute fossils preserved by apatite and glauconite (Pruss *et al.* 2018). These assemblages contain small fossils of groups that had been described previously, including many echinoids, gastropods and rare foraminifera (e.g. Schubert & Bottjer 1995). The fossils were found in samples that had been previously examined for their silicified faunas, but these apatitic and glauconitic fossils were found in the smallest size fractions only (between 177 and 420 μm) (Pruss *et al.* 2018), confirming the notion that small size influences the nature of preservation (Creveling *et al.* 2014a, 2014b).

Here we describe a new assemblage from the Virgin Limestone Member of the western United States at the Lost Cabin Springs (LCS) locality, an exposure of the Virgin Limestone that records a more distal setting than the units exposed in the Muddy Mountains (Pruss *et al.* 2005a; Pruss *et al.* 2005b). We report silicified/dolomitized fossils in the larger size fractions; however, the majority of the fossils that are $<1000 \mu\text{m}$ are phosphatized, indicating that this style of preservation was occurring broadly across the Early Triassic shelf in the western United States. Whilst we report and describe the silicified and dolomitized components of this assemblages, this paper focuses on phosphatization and aims to compare the two occurrences of SSF preservation found in different depositional environments of the Lower Triassic Virgin Limestone Member to add to our understanding of small shelly-style fossil preservation more broadly.

The fossils recovered from LCS samples are similar to those from Muddy Mountains in that they preserve fossils that had been described previously from macrofossil assemblages, but unlike Muddy Mountains, the LCS assemblages contain brachiopods, a more diverse array of gastropods, a single bivalve and two ostracods. Similar to Muddy Mountains, echinoid spines and crinoids are also recovered. Ophiuroid fragments are incredibly abundant in one sample but were found in no others. Additionally, no fossils were preserved by glauconite in LCS assemblages, which was a common replacement or internal moulding mineral at Muddy Mountains. The variability of fossils between assemblages at these two localities points to local controls on diversity but broadly similar, and widespread, taphonomic conditions across the Early Triassic shelf.

Geological setting

During the Permian and Triassic, the Panthalassa sea flooded present-day southwestern North America (e.g. Marzolf 1993; Pruss *et al.* 2005a). Sedimentation was, however, discontinuous across western North America during the Permo-Triassic, with only a few boundary sections known (Alvarez & O'Connor 2002; Sperling & Ingle 2006). By the later Early Triassic, the Moenkopi Formation was deposited on a broad shallow epicontinental shelf that extended from southern Idaho to southern Arizona (Marzolf 1993). Moenkopi strata record the waxing and waning of the epicontinental sea in non-marine or marginally marine redbeds and nearshore to middle-shelf siliciclastics and carbonates (e.g. Shorb 1983).

The uppermost lower Triassic (Spathian) Virgin Limestone Member of the Moenkopi Formation has been studied extensively, both for the various microbialites it preserves (Mata & Bottjer 2011; Pruss *et al.* 2004; Schubert & Bottjer 1992) and its faunas, which reflect recovery from the end-Permian mass extinction (Schubert and Bottjer, 1995; Fraiser & Bottjer 2007; Hoffmann *et al.* 2013; McGowan *et al.* 2009; Pruss *et al.* 2018). The mixed carbonate-siliciclastic Virgin Limestone is composed of limestone, dolomitic limestone, calcareous mudstone and siltstone (Reif & Slatt 1979) and contains fossil material such as echinoderm debris, bivalves, gastropods (e.g. Schubert & Bottjer 1992; Schubert & Bottjer 1995; Hoffmann *et al.* 2013) and ophiuroids (Twitchett *et al.* 2005). It was deposited in a storm-dominated subtidal palaeoenvironment (e.g. Poborski 1954; Stewart *et al.* 1972; Pruss *et al.* 2005b) as a transgressive marine tongue from Panthalassa.

At the Lost Cabin Springs locality in southern Nevada (Fig. 1), the Virgin Limestone Member overlies the Lower Red Member and is conformably overlain by the evaporitic Shnabkaib Member (e.g. Stewart *et al.* 1972; Marzolf 1993; Pruss *et al.* 2005a). Here, the lowest exposed beds consist largely of siliciclastic sediments; carbonate beds become more common and thicker higher in the exposed section (Fig. 2). The Virgin Limestone exposed at the Lost Cabin Springs locality records carbonate-dominated subtidal shelf palaeoenvironments, deeper than coeval sections in the Muddy Mountains (Pruss *et al.* 2005b).

Methods

For this work, following on the sampling scheme of Pruss *et al.* (2018), we sampled limestone beds that had silicified fossils present in hand samples. In

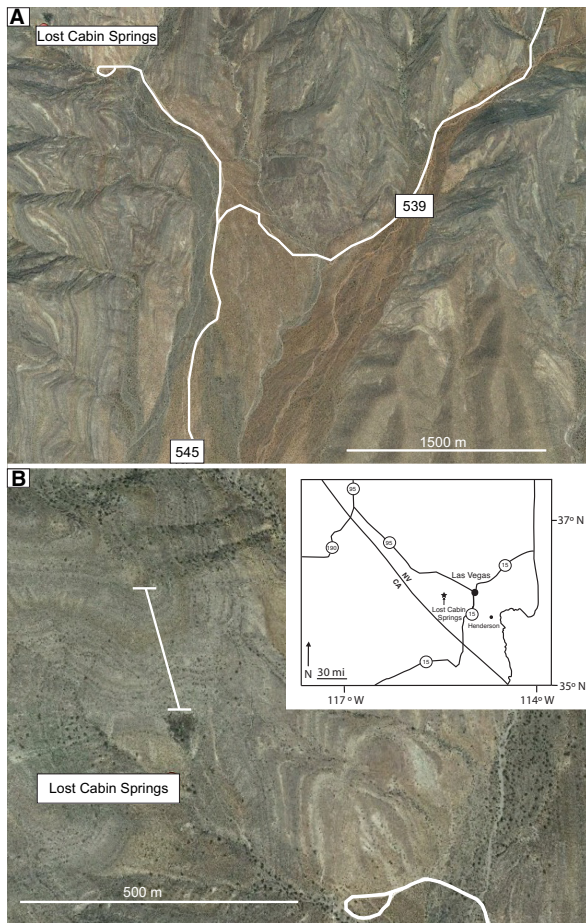


Fig. 1. Map showing location of the outcrops of the Virgin Limestone Member at the Lost Cabin Springs Locality in Southern Nevada, ~30 miles west of Las Vegas, NV, western United States (36°4'57.18'N, 115°39'12.05'W is near the base of the section). Downloaded from <https://maps.google.com/>. [Colour figure can be viewed at [wileyonlinelibrary.com](https://onlinelibrary.wiley.com)]

previous work, these beds tended to produce abundant fossils in insoluble residues, only some of which were silicified. Ten samples of fossiliferous packstone from Lost Cabin Springs were collected over a ~125 m of section in two field seasons. All ten samples were dissolved in 200–400 mL of 10% glacial acetic acid solution buffered with ammonium acetate. The samples were sieved and insoluble residues >400 μm, >250 μm and >177 μm were collected. These residues were picked for fossils under the Nikon SMZ645 stereoscopic microscope. Only eight samples produced abundant fossils though the diversity and abundance varied between samples; only these fossiliferous residues were considered in further analyses. The fossils were imaged using the Olympus BHS BH-2 Light Microscope. After light images were captured, the fossils were coated with gold and palladium by a Hummer V Sputter coater and imaged with the FEI Quanta 450 Scanning Electron Microscope (SEM) at Smith College. EDS (Energy-

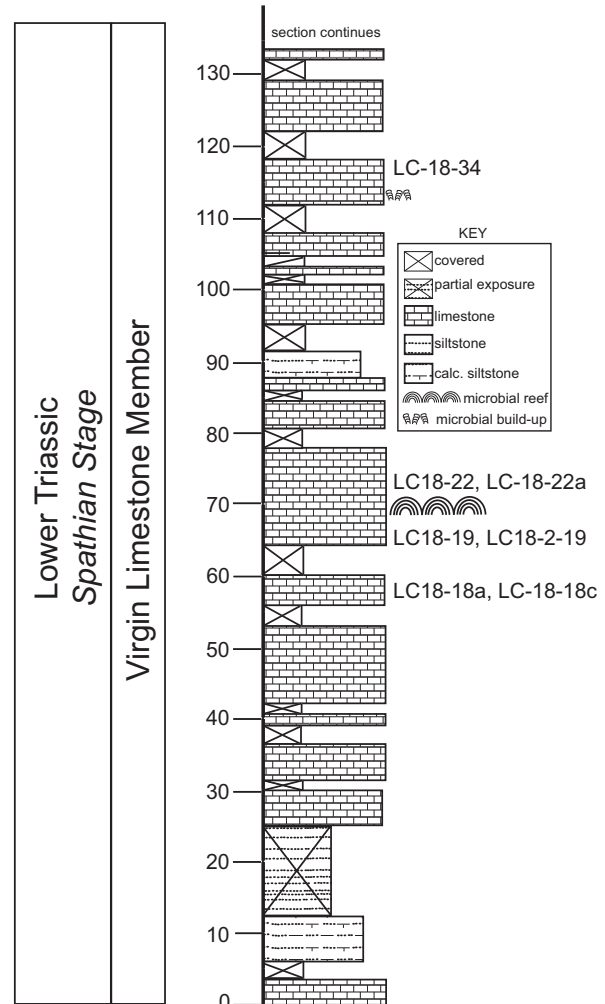


Fig. 2. Partial graphical column of the Virgin Limestone Member at Lost Cabin Spring where samples were collected; all labelled beds produced fossils and correspond to bed names in Table 1.

Dispersive Spectroscopy) Team software was also used to analyse the elemental composition of 119 fossils. Finally, SEM images of individual fossils in this work were measured (length of brachiopods, width of echinoid spines, width of crinoid ossicles, long axis of gastropods and width of ophiuroid elements) to determine the range of sizes preserved in each group of fossils, though only some SEM images were suitable for measurement. For example, brachiopods, though abundant in residues overall, did not have many SEM images that could be accurately measured.

Results

Field and sample observations

Five beds (LC-18-18, LC-18-19, LC-18-22, LC-18-34 and LC-18-35) were sampled from the Virgin

Limestone Member of the Moenkopi Formation at Lost Cabin Springs, but the sample from LC-18-35 had very few fossils so was not considered further in this analysis (Fig. 2; Table 1). LC-18-19 was sampled during two different field seasons (LC-18-19 and LC-18-2-19), and beds LC-18-18 and LC-18-22 yielded three samples and two samples respectively (LC-18-18a, LC-18-18b, LC-18-18c, LC-18-22 and LC-18-22a). Of these, LC-18-18b had rare fossils so was excluded from analysis. A total of eight samples were thus considered further in this work. The beds were identified for sampling based on facies previously described in Pruss (2004) as having silicified fossils, the residues of which produced glauconitized and phosphatized fossils in previous work (Pruss *et al.* 2018).

Packstones with previously noted silicified fossils were sampled in this work (Table 1). Only larger macrofossils are apparent in hand samples – these include crinoids and echinoid spines. Large calcareous gastropods and bivalves were present in some Virgin beds but were not visible in hand samples that produced abundant small shelly-style fossils in residue. The lowermost bed sampled in this work is Bed LC-18-18, a 5-m-thick bed with the lower 1.5 m consisting of limestone with thin silty intercalations with *Thalassinoides* at the top of the 1.5 m and overlain by a packstone/grainstone with abundant crinoidal debris, ooids and intraclasts. Bed LC-18-19 is a crinoidal packstone with horizontal trace fossils preserved on top. Bed LC-18-22 is a ~7 m-thick fossiliferous packstone with prominent echinoid spines (Moffat & Bottjer 1999) that overlies a well-studied microbial reef horizon (Schubert & Bottjer 1992; Pruss *et al.* 2004). Two samples were taken from this thick bed and reveal slightly different fossil assemblages: gastropods were abundant in LC-18-22 insoluble residues, whereas crinoids and echinoids were the common fossils in LC-18-22a both in the packstone and in insoluble residues. Bed LC-18-34 is

a ~0.5 m-thick packstone of crinoidal debris and intraclasts; it sits 0.2 m above another prominent stromatolitic unit, but one that is much smaller than the reef horizon. Bed LC-18-34 was the only unit to contain ophiuroids, which were found in abundance only in insoluble residues. Gastropods were also present in the insoluble residues of this bed.

Insoluble residue observations

Eight samples from the Lost Cabin Springs locality contain a greater diversity than those at the Muddy Mountains locality. The smallest fossils in our assemblages are internal moulds of brachiopods, internal moulds of gastropods, a single occurrence of an internal mould of a bivalve and two replaced ostracods (Fig. 3). The majority of these fossils are <1000 µm. Echinoderms are common in LCS assemblages (Fig. 4), and most crinoid ossicles are the largest fossils, with all but 1 > 1000 µm. Echinoid spines and ophiuroids are smaller than the crinoids (all <1000 µm), and all echinoderms are preserved as stereomic moulds. Some fossils were unique to one sample, such as abundant ophiuroid fragments preserved only in LC-18-34, and two occurrences of ostracods found in LC-18-18c (Table 1). Brachiopods were found in 5 samples, but their abundance varied.

Measurements of 120 SEM images of fossils yielded important size distribution data for different groups preserved in our assemblages (Fig. 5, Table S1). Brachiopods range in size from 104 to 250 µm, and the width of echinoid spines range from 57 to 268 µm. Gastropods and ophiuroid elements are generally larger; the former has a range from 230 to 873 µm, and the latter is 242 to 923 µm. Crinoid ossicles range from 938 µm to 2523 µm and are the largest fossils measured in the residues. The size range of crinoid ossicles does not overlap with any fossils that are phosphatized.

Table 1. Table showing sample names, facies descriptions, common fossils in insoluble residues and minerals preserving the fossils

Sample	Facies	Minerals	Fossils
LC-18-18a, 18c	crinoidal grainstone/packstone with <i>Thalassinoides</i>	Apatite, silica; iron-bearing minerals	brachiopods; echinoid spines; gastropods; ostracods
LC-18-19, LC-18-2-19	crinoidal packstone with horizontal bioturbation preserved on top	Apatite; silica; iron-bearing minerals	brachiopods; crinoids; echinoid spines; gastropods; bivalve
LC-18-22, 22a	limestone ledge overlying microbial mounds, grainy in places, contains echinoid spines, muddier at base, grainer near the top, silicified fossils	Apatite; silica; dolomite; iron-bearing minerals	brachiopods, gastropods
LC-18-34	thick packstone with crinoidal debris, some rip-ups, some bioturbation preserved on top of muddy surfaces	Apatite; silica	ophiuroids, gastropods, echinoids

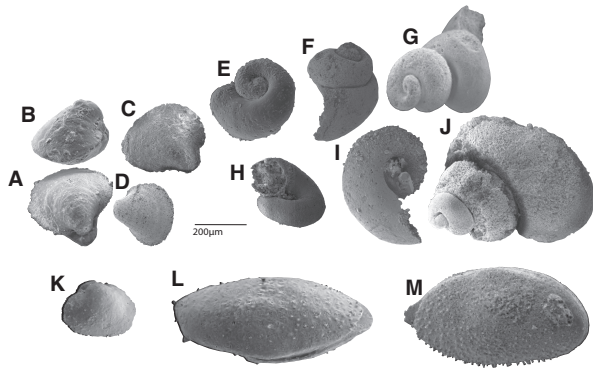


Fig. 3. Common phosphatized fossils. Internal moulds of the brachiopod *Protogusarella smithi* (A–D), internal moulds of gastropods (E–J), internal mould of a bivalve, possibly *Sementiconcha recuperator* (K) and phosphatized ostracods (L, M).

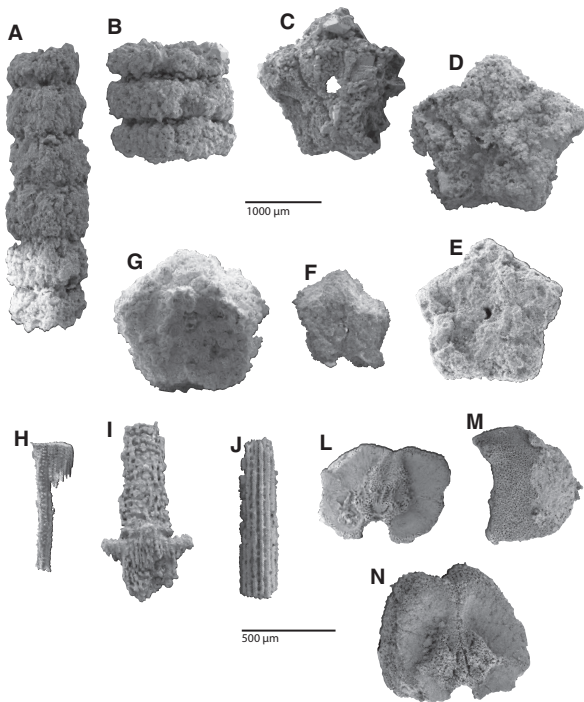


Fig. 4. Echinoderm fragments. Silicified stereomic moulds of *Holocrinus smithi* crinoids (A–G), phosphatized stereomic moulds of echinoid spines belonging to Miocidaridae (H–J), phosphatized stereomic moulds of a new species of ophiuroids (L–N).

EDS analysis of Lost Cabin Springs fossils

Unlike the fossils at the Muddy Mountains locality (Pruss *et al.* 2018), no fully glauconitic fossils were found in Lost Cabin Springs residues. The EDS analysis of 119 fossils shows that there is some variability in the minerals of the fossils (Fig. 6). Ophiuroids and brachiopods (Fig. 6A, B) showed peaks in Ca, P and O, with the brachiopod showing a small F peak, confirming a composition of calcium-fluorapatite.

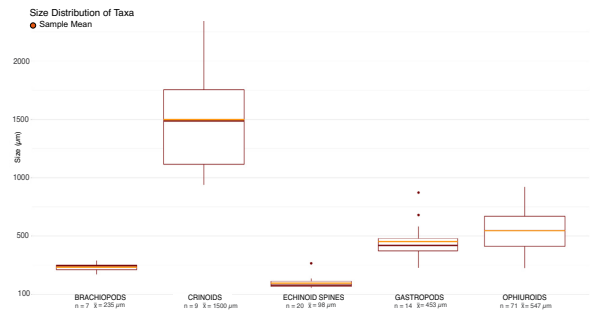


Fig. 5. Graph showing sizes of common fossils in insoluble residues measured from SEM images. Sizes were determined by measuring the length of brachiopods, width of echinoid spines, width of crinoid ossicles, long axis of gastropods and width of ophiuroid elements. [Colour figure can be viewed at wileyonlinelibrary.com]

Fluoride is also present in some ophiuroids, gastropods and a bivalve, and is therefore not unique to brachiopods. The larger crinoids (>1000 µm) contain abundant Si and O (Fig. 6C) suggesting silica as a dominant replacement mineral. Other crinoids revealed peaks in Ca and Mg, consistent with dolomite. Fe is occasionally present in some EDS point analyses; for example, in one EDS point analysis of an internal mould of a gastropod, Fe, Mg, K, Si, Al and O were found, suggesting the presence of glauconite, but overall, glauconite was rare in these assemblages. The smallest size fractions (<1000 µm) are dominated by phosphatized fossils, confirmed by EDS. There was also an observed difference in colour and texture between phosphatized and silicified specimens in residue: the phosphatized fossils had a brownish colour whereas the silicified fossils were yellowish/white.

Discussion

Virgin Limestone palaeoenvironments and palaeoecology at Lost Cabin Springs

The Spathian Moenkopi Formation was deposited on the Colorado Plateau, and the Virgin Limestone Member represents a marine incursion during Early Triassic time (Marzolf 1993). The Virgin Limestone Member was deposited in intertidal to mid-shelf palaeoenvironments and is exposed from eastern California to southwestern Utah (Stewart *et al.* 1972; Marzolf 1993; Shorb 1983). The Lost Cabin Springs section represents carbonate-dominated inner to middle-shelf palaeoenvironments (Schubert & Bottjer 1995; Pruss *et al.* 2005a; Mata & Bottjer 2011), a slightly thicker and deeper exposure of the Virgin Limestone Member than the exposures in the Muddy Mountains.

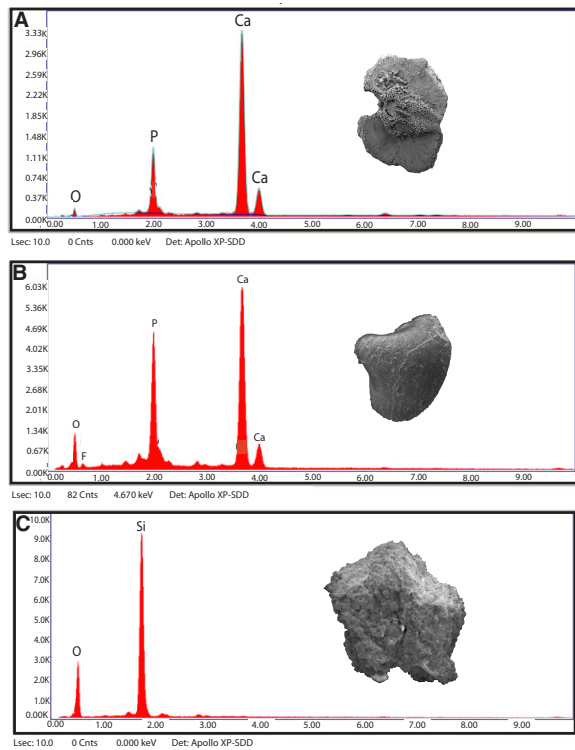


Fig. 6. Energy-Dispersive Spectra (EDS) analysis showing abundance of elements in common fossils. A, EDS of an ophiuroid from bed LC-18-34 showing peaks of Ca, P, and O. B, EDS of a brachiopod from bed LC-18-22a showing high abundance of Ca, P and O, with trace F. C, EDS of crinoid ossicle from bed LC-18-19 showing high abundance of Si and O. [Colour figure can be viewed at wileyonlinelibrary.com]

Previous work demonstrated that environments in the Virgin Limestone range from shallow subtidal wave-dominated settings to deeper water storm-dominated settings, with occasional deposition below storm wave base (Schubert & Bottjer 1995; Pruss *et al.* 2005a; Pruss *et al.* 2005b). Schubert & Bottjer (1995) identified several palaeocommunities within the Virgin Limestone, all characterized by abundant bivalves and distinguished by the ancillary organisms. Fraiser & Bottjer (2007) also showed bivalve dominance in most Lower Triassic sections of the western United States, including within the Virgin Limestone. Interestingly, bivalves make up a very small proportion of the fossils in our assemblages. Our assemblages are dominated by juvenile brachiopods, echinoderms and gastropods, again pointing to the importance of the size of organisms in phosphatization rather than their original abundances.

Analysis of macrofossils found in previous work on the Virgin Limestone Member include bivalves, gastropods, echinoderms, ophiuroids, and rare ammonoids (e.g. Poborski 1954; Shorb 1983; Stewart

et al. 1972; Schubert & Bottjer 1995, Hoffmann *et al.* 2013). Our samples reveal the presence of similar organisms, though residue abundances do not always match those in macrofossil assemblages, as has been shown in other studies of the Virgin Limestone (Pruss *et al.* 2018). Brachiopods, crinoids, echinoid spines, gastropods, ophiuroids, rare bivalves and two ostracods are the components of our assemblages (Figs 3, 4). The lack of preservation of meaningful morphological traits make it difficult to determine whether echinoderms and gastropods are adults or juveniles.

The diversity of fossils in the LCS insoluble residue assemblages reflects what is known from macrofossil assemblages with the exception of a new ophiuroid species. LCS juvenile brachiopods belong to *Protogusarella smithi* (Fig. 3A–D). The fossils depicted in Figures 3A–D have symmetry consistent with brachiopods, and there is consistency between the specimens in terms of shape and size, though there are taphonomic effects that alter how some brachiopods appear under the SEM. Crinoid specimens are remnants of *Holocrinus smithi* (Fig. 4A–G). The echinoid spines (Fig. 4H–J) belong to an echinoid from the family Miocidaridae (Kier 1968; Moffat & Bottjer 1999) but are an undetermined genus and species (Rolle 2014). A previously undocumented species of ophiuroids are present in LC-18-34 (Fig. 4L–N), and are likely closely related to the *Praeaplocoma hessi* from the Lower Triassic of Italy. Planispiral and high-spired gastropods are also common components of our assemblage (Fig. 3E–J), but as these are preserved as internal moulds, and thus lack surface ornamentation, no further identification of them is possible. There is one occurrence of a poorly preserved internal mould of a bivalve, likely belonging to *Sementiconcha recuperator* (Fig. 3K) (Hautmann *et al.* 2013), and two occurrences of ostracods (Fig. 3 L, M). Unlike Cambrian SSFs, the Lost Cabin Springs assemblage does not reveal a diversity of organisms that is significantly different from the macrofossil assemblages, but some features of these minute fossils, such as the ophiuroid fragments, will make it possible to identify new species in these assemblages that would have passed unnoticed otherwise.

Taphonomy of assemblages at Lost Cabin Springs

The Lost Cabin Springs section provides evidence of deposition in a storm-dominated subtidal palaeoenvironment (Schubert & Bottjer 1995; Pruss *et al.* 2005b), but questions remain about whether or not this influenced phosphatization. Freeman *et al.* (2019) report that the majority of millimetre-scale,

steinkern-yielding, phosphorite-rich beds are associated with signs of low sedimentation rates, or sedimentary hiatuses, and that no cases were reported in areas where ongoing rapid or even normal sedimentation occurred (Table 1; Freeman *et al.* 2019). High-energy mixing events – such as storms – may bury live or recently dead benthic organisms (e.g. Freeman *et al.* 2013; Milam *et al.* 2017), which is argued to enhance phosphogenesis. As the organic matter decays, organic-bound phosphorus is rapidly released. This release enhances interstitial phosphorus content, whilst accommodating increased calcium-fluorapatite (CFA) precipitation by enhancing the volume of sediment encompassed by the complex of small redox zones around areas of decaying matter (e.g. Aller 1982; Föllmi 1990, 1996; Föllmi & Garrison 1991). These zones can increase the volume of sediment in the zone of phosphatization, thus enhancing CFA precipitation in areas of high-energy mixing events. This model was developed in part to argue that CFA precipitation is more widespread in the geological record than previously suspected and can occur under common conditions (Freeman *et al.* 2019).

Indeed, most of the apatite fossil-bearing beds at Lost Cabin Springs are likely storm deposits, particularly Bed 22, a well-studied echinoid spine deposit (Moffat & Bottjer 1999). This thick bed was previously interpreted as a storm bed and the majority of spines ranging from 1 to 6 mm were silicified (Moffat & Bottjer 1999), as were the crinoids found in our insoluble residue assemblage. However, phosphatized fossils, while present, are not particularly prevalent in this unit. Furthermore, the spines show evidence for disarticulation and abrasion, suggesting significant reworking, which likely minimized the effective burial of recently dead organisms and their organic matter. And, as in previous Triassic examples (Pruss *et al.* 2018), there are no phosphatic hardgrounds or other evidence for widespread concentrations of phosphatized grains or layers. It seems unclear that phosphate concentration via reworking operates as the primary mechanism for fossilization in most Virgin Limestone beds.

Size selectivity and phosphatization

A potential link between small shells and enhanced phosphate precipitation for both Cambrian (Yochelson 1999; Creveling *et al.* 2014a; Jacquet & Brock 2016) and non-Cambrian occurrences (Lamboley 1987, 1993; Datillo *et al.* 2016) has been proposed. In previous work, Pruss *et al.* (2018) suggested a size selectivity of taphonomic processes preserving Triassic phosphatic and glauconitic steinkerns that were

related to particle radius and O₂ consumption. Our work here supports similar size selectivity. In measurements of SEM images of fossils that were common in our residues, the range in size of phosphatized fossils is smaller and does not overlap with the sizes of silicified fossils (Fig. 5). All measured phosphatized fossils in LCS assemblages are on average smaller than the silicified crinoids. Crinoids range in size from ~1 to ~2.5 mm whereas none of the phosphatized brachiopods, gastropods, echinoids or ophiuroids had dimensions as long as 1 mm, and all had average sizes of ~550 µm or less. The strongest predictor of phosphatization in LCS assemblages is not original skeletal material nor abundance, but size.

The mechanisms for phosphatization of small fossils are likely variable and related to a host of environmental conditions. In all cases, whilst there may be some common and recurring depositional settings that lend themselves to phosphatization, it is not clear that phosphatization is truly ubiquitous in the fossil record. However, it is also clear that phosphatization is not isolated to the Cambrian (e.g. Dzik 1994; Pruss *et al.* 2018; Datillo *et al.* 2019; Freeman *et al.* 2019). What can be learned from two occurrences of small shelly fossil-style preservation in Lower Triassic sediments in different subtidal settings?

Modern studies point to redox oscillations as controllers of availability of oxidants particularly in pore water pH (Zhu *et al.* 2006), linking low pore water SO₄²⁻ to the formation of apatite. For example, along the East Australian continental margin (O'Brien *et al.* 1990), high organic carbon delivery creates low-oxygen conditions, and iron and phosphorus cycling can increase local concentrations of phosphorus; interestingly, some iron minerals act as more effective P shuttles than others, which relates to adsorption sites and surface area (Creveling *et al.* 2014a). For example, iron oxyhydroxides are thought to be incredibly efficient at adsorbing phosphate from seawater (Feely *et al.* 1991, 1998; Peacock *et al.* 2016) and delivering it to sediments.

The role of iron in Lost Cabin Springs sediments is unclear, though one sample of insoluble residues yielded sparse pyrite grains (LC-18-22a), suggesting local reducing conditions, at least some of the time. Glauconite is far less abundant in these samples as grains and as a replacement and moulding fossil mineral compared to the Muddy Mountains assemblages (Pruss *et al.* 2018). Much like most Lower Triassic sediments, the total organic carbon (TOC) is low in Lost Cabin Springs strata (Marenco *et al.* 2012), so it seems clear that in this case, excess organic matter did not contribute significantly to

local phosphorus accumulation. And, as shown in previous work, it is unlikely that enough organic matter existed in the recently dead organisms themselves to account for their phosphatization (Creveling *et al.* 2014a, 2014b).

Here, we prefer a mechanism in which the small particle size of the organisms coupled with an ambient pore water environment that experienced periodic oscillations in oxygen fostered phosphatization of minute shells. The Early Triassic ocean is thought to have been exceedingly warm (e.g. Sun *et al.* 2012), which is coupled with (and likely related to) extensive evidence for low-oxygen conditions (e.g. Isozaki 1997; Grice *et al.* 2005; Grasby *et al.* 2013; Song *et al.* 2014; Pietsch *et al.* 2016). Furthermore, these sections are well known for the absence of deeply penetrating burrows, and many beds contain very little overall bioturbation (Pruss & Bottjer, 2004), which may have also acted to minimize the introduction of oxygen into the sediments. The unique depositional environments of the Early Triassic likely contributed to the glauconitization and phosphatization seen in Virgin Limestone assemblages. No fossils larger than 1000 μm are preserved by apatite in our assemblages – larger fossils, in this case crinoids, are preserved as stereomic moulds of silica and dolomite, and often in the same samples where phosphatization is occurring. This again points to a complex taphonomic history in which some fossils are replaced or moulded by silica (crinoids) whilst others, even with a similar skeletal composition of high-Mg calcitic stereom (e.g. ophiuroids and echinoids), are phosphatized. In Ediacaran assemblages that contain both phosphatic and siliceous fossils, many Ediacaran fossils can be preserved by both pathways, but the environments of deposition are slightly different (e.g. Muscente *et al.* 2014). That the same diagenetic environment in Lower Triassic units can lead to different minerals replacing fossils within the same bed reiterates that the pore water environment and size of shells must be the two most important factors governing silicification and phosphatization of LCS fossils (e.g. Pruss *et al.* 2018), in both nearshore and more offshore settings.

Conclusions

The occurrence of small shelly-style preservation in samples from the Virgin Limestone Member shows that this style of preservation was occurring broadly across the Early Triassic shelf of eastern Panthalassa. Whilst the majority of our LCS samples reflect deposition in a distal and storm-dominated subtidal palaeoenvironment, we argue that local pore water

redox controls on the sediments – which allow for the accumulation of phosphorus – played a more significant role in their preservation than phosphate concentration via reworking. The size selectivity of phosphatization is evident, as the smallest size fraction predominantly contained phosphatized fossils, whereas larger fossils extracted in insoluble residues were replaced or moulded by silica and dolomite. There were rare occurrences of bivalves and ostracods present in our samples, despite the well documented numerical dominance of bivalves in shallow level-bottom benthic marine communities. This further illustrates that the size of fossils more directly controls the nature and distribution of phosphatization than their initial abundance in ancient communities. It is possible that more searching for SSF-style preservation in sediments of other ages will yield additional occurrences; however, the mechanism(s) for their formation, whilst present through time, may be related to many and variable environmental factors. The Early Triassic shallow marine realm seems particularly well suited to the formation of SSF-style fossils, with warm, low-oxygen seas persisting until Middle Triassic time.

Acknowledgements. – We acknowledge E. Smith, O. Leadbetter, T. McGann, R. Revolorio Keith, M. Slaymaker and A. Hagen for help in field collection. We thank C. Stark for field assistance and initial analysis of the samples. We thank Smith Geosciences for generous funding for this project, and P. Wignall for thoughtful conversations about this work.

References

- Aller, R.C. 1982: The effects of macrobenthos on chemical properties of marine sediment and overlying water. In McCall, P.L. & Tevesz, M.J.S. (eds): *Animal-Sediment Relations: The Biogenic Alteration of Sediments*, 53–102. Plenum Press, New York.
- Alvarez, W. & O'Connor, D. 2002: Permian-Triassic boundary in the southwestern United States: Hiatus or Continuity? In Koeberl, C. & MacLeod, K.G. (eds): *Catastrophic Events and Mass Extinctions: Impacts and Beyond Geological Society of America Special Papers 356, Boulder*, 385–393.
- Brasier, M.L. 1990: Phosphogenic events and skeletal preservation across the Precambrian-Cambrian boundary interval. *Geological Society of London, Special Publications 52*, 289–303.
- Creveling, J.C., Johnston, D.T., Poulton, S.W., Kotrc, B., Marz, C., Schrag, D.P. & Knoll, A.H. 2014a: Phosphorus sources for phosphatic Cambrian carbonates. *Geological Society of America Bulletin 126*, 145–163.
- Creveling, J.C., Knoll, A.H. & Johnston, D.J. 2014b: Taphonomy of Cambrian small shelly fossils. *Palaios 29*, 295–308.
- Datillo, B.F., Freeman, R.L., Peters, W.P., Heimbrock, W.P., Deline, B., Martin, A.M., Kallmeyer, J.W., Reeder, J. & Argast, A. 2016: Giants among micromorphs: were Cincinnatian (Ordovician, Katian) small shelly phosphatic faunas dwarfed? *Palaios 31*, 55–70.
- Datillo, B.F., Freeman, R.L., Zubovic, Y.M., Brett, C.E., Straw, A.M., Frauhiger, M.J., Harstein, A.R. & Shoemaker, M.L. 2019: Time-richness and phosphatic microsteinkern accumulation in the Cincinnatian (Katian) Ordovician, USA: an example of

- polycyclic phosphogenic condensation. *Palaeogeography, Palaeoclimatology, Palaeoecology* 535, 109362.
- Dzik, J. 1994: Evolution of 'small shelly assemblages' of the early Paleozoic. *Acta Palaeontologica Polonica* 39, 247–313.
- Feely, R.A., Trefry, J.H., Lebon, G.T. & German, C.R. 1998: The relationship between P/Fe and V/Fe ratios in hydrothermal precipitates and dissolved phosphate in seawater. *Geophysical Research Letters* 25, 2253–2256.
- Feely, R.A., Trefry, J.H., Massoth, G.J. & Metz, S. 1991: A comparison of the scavenging of phosphorus and arsenic from seawater by hydrothermal iron oxyhydroxides in the Atlantic and Pacific Oceans. *Deep-Sea Research* 38, 617–623.
- Föllmi, K.B. 1990: Condensation and phosphogenesis: examples of the Helvetic mid-Cretaceous (northern Tethyan margin). In Notholt, A.J.G. & Jarvis, I. (eds): *Phosphorite Research and Development. Geological Society Special Publication* 52, 237–252.
- Föllmi, K.B. 1996: The phosphorus cycle, phosphogenesis and marine phosphate-rich deposits. *Earth Science Reviews* 40, 55–124.
- Föllmi, K.B. & Garrison, R.E. 1991: Phosphatic sediments, ordinary or extraordinary deposits? The example of Miocene Monterey Formation (California). In Muller, D.W., McKenzie, J.A. & Weissert, H. (eds): *Phosphatic sediments, ordinary or extraordinary deposits? The example of Miocene Monterey Formation (California)*, 55–84. Controversies in Modern Geology. Academic Press, London.
- Fraiser, M.L. & Bottjer, D.J. 2007: When bivalves took over the world. *Paleobiology* 33, 397–413.
- Freeman, R.L., Dattilo, B.F. & Brett, C.E. 2019: An integrated stratigraphic model for the genesis and concentration of 'small shelly fossil'-style phosphatic microsteinkerns in not-so-exceptional conditions. *Palaeogeography, Palaeoclimatology, Palaeoecology* 535, 109344.
- Freeman, R.L., Dattilo, B.F., Morse, A., Blair, M., Felton, S. & Pojeta, J. 2013: The 'Curse Of Rafinesquina': negative taphonomic feedback exerted by strophomenid shells on storm-buried Lingulids in The Cincinnati Series (Katian, Ordovician) of Ohio. *Palaiois* 28, 359–372.
- Grasby, S.E., Beauchamp, B., Embry, A. & Sanei, H. 2013: Recurrent Early Triassic anoxia. *Geology* 41, 175–178.
- Grice, K., Cao, C., Love, G.D., Böttcher, M.E., Twitchett, R.J., Grosjean, E., Summons, R.E., Turgeon, S.C., Dunning, W. & Jin, Y. 2005: Photic zone euxinia during the Permian-Triassic superanoxic event. *Science* 307, 706–709.
- Hautmann, M., Smith, A.B., McGowan, A.J. & Bucher, H. 2013: Bivalves from the Olenekian (Early Triassic) of south-western Utah: systematics and evolutionary significance. *Journal of Systematic Palaeontology* 11, 263–293.
- Hoffmann, R., Hautmann, M., Wasmer, M. & Bucher, H. 2013: Palaeoecology of the Spathian Virgin Formation (Utah, USA) and Its Implications for the Early Triassic Recovery. *Acta Palaeontologica Polonica* 58, 149–173.
- Isozaki, Y. 1997: Permo-Triassic boundary superanoxia and stratified superocean; records from lost deep sea. *Science* 276, 235–238.
- Jacquet, S.M. & Brock, G.A. 2016: Lower Cambrian helcionelloid macromolluscs from South Australia. *Gondwana Research* 36, 333–358.
- Kier, P.M. 1968: The Triassic Echinoids of North America. *Journal of Paleontology* 4, 1000–1006.
- Lamboy, M. 1987: Genèse de grains de phosphate à partir de débris de squelette d'échinodermes: les processus et leur signification. *Bulletin de la Société Géologique de France, series* 8(3), 759–768.
- Lamboy, M. 1993: Phosphatization of calcium carbonate in phosphorites: microstructure and importance. *Sedimentology* 40, 53–62.
- Marengo, P.J., Griffin, J.M., Fraiser, M.L. & Clapham, M.E. 2012: Paleocology and geochemistry of Early Triassic (Spathian) microbial mounds and implications for anoxia following the end-Permian mass extinction. *Geology* 40, 715–718.
- Marzolf, J.E. 1993: Palinspastic reconstruction of early Mesozoic sedimentary basins near the latitude of Las Vegas; implications for the early Mesozoic Cordilleran cratonal margin. *Mesozoic Palaeogeography of the Western United States; II* 71, 433–462.
- Mata, S.A. & Bottjer, D.J. 2011: Origin of Lower Triassic microbialites in mixed carbonate-siliciclastic successions: Ichology, applied stratigraphy, and the end-Permian mass extinction. *Palaeogeography, Palaeoclimatology, Palaeoecology* 300, 158–178.
- McGowan, A.J., Smith, A.B. & Taylor, P.D. 2009: Faunal diversity, heterogeneity and body size in the Early Triassic: testing post-extinction paradigms in the Virgin Limestone of Utah, USA. *Australian Journal of Earth Sciences* 56, 859–872.
- Milam, M.J., Meyer, D.L., Dattilo, B.F. & Hunda, B.R. 2017: Taphonomy of an Ordovician crinoid lagerstätte from Kentucky. *Palaiois* 32, 166–180.
- Moffat, H.A. & Bottjer, D.J. 1999: Echinoid concentration beds: two examples from the stratigraphic spectrum. *Palaeogeography, Palaeoclimatology, Palaeoecology* 149, 329–348.
- Muscante, A.D., Hawkins, D. & Xiao, S. 2014: Fossil preservation through phosphatization and silicification in the Ediacaran Doushantuo Formation (South China): a comparative synthesis. *Palaeogeography, Palaeoclimatology, Palaeoecology* 2014, 46–62.
- O'Brien, G.W., Milnes, A.R., Veeh, H.H., Heggie, D.T., Riggs, S.R., Cullen, D.J., Marshall, J.F. & Cook, P.J. 1990: Sedimentation dynamics and redox iron-cycling: controlling factors for the apatite-glaucinite association on the east Australian continental margin. In Notholt, A.J.G. & Jarvis, I. (eds): *Phosphorite Research and Development*, volume 52, 61–86. Geological Society Special Publication, London.
- Peacock, C.L., Lalonde, S. & Konhauser, K.O. 2016: Iron minerals as archives of Earth's redox and biogeochemical evolution. *EMU Notes in Mineralogy* 17, 113–164.
- Pietsch, C., Petsios, E. & Bottjer, D.J. 2016: Sudden and extreme hyperthermals, low-oxygen, and sediment influx drove community phase shifts following the end-Permian mass extinction. *Palaeogeography, Palaeoclimatology, Palaeoecology* 451, 183–196.
- Poborski, S.J. 1954: Virgin Formation (Triassic) of the St. George, Utah, area. *Geological Society of America Bulletin* 65, 971–1006.
- Porter, S.M. 2004: Closing the phosphatization window: testing for the influence of taphonomic megabias on the pattern of small shelly fossil decline. *Palaiois* 19, 178–183.
- Pruss, S.B. 2004: The unusual sedimentary rock record of the Early Triassic: anachronistic facies in the Western United States and Southern Turkey. Ph.D Thesis, University of Southern California, Los Angeles, CA, 286 pp.
- Pruss, S.B. & Bottjer, D.J. 2004: Early Triassic trace fossils of the western United States and their implications for prolonged environmental stress from the end-Permian mass extinction. *Palaiois* 19, 559–571.
- Pruss, S.B., Corsetti, F.A. & Bottjer, D.J. 2005a: The unusual sedimentary rock record of the Early Triassic: a case study from the southwestern United States. *Palaeogeography, Palaeoclimatology, Palaeoecology* 222, 33–52.
- Pruss, S.B., Corsetti, F.A. & Bottjer, D.J. 2005b: Environmental trends of Early Triassic biofabrics: implications for understanding the aftermath of the end-Permian mass extinction. In Morrow, J. D., Over, D. J. & Wignall, P.B. (eds): *Understanding Late Devonian and Permian-Triassic Biotic and Climatic Events: Towards and Integrated Approach*, 313–332, Developments in Palaeontology and Stratigraphy, Elsevier, Berlin.
- Pruss, S.B., Fraiser, M.L. & Bottjer, D.J. 2004: Proliferation of Early Triassic wrinkle structures: implications for environmental stress following the end-Permian mass extinction. *Geology* 35, 461–465.
- Pruss, S.B., Tosca, N.J. & Courcelle, S. 2018: Small shelly fossil preservation and the role of early diagenetic redox in the Early Triassic. *Palaiois* 33, 441–450.
- Reif, D.M. & Slatt, R.M. 1979: Red bed members of the Lower Triassic Moenkopi Formation, southern Nevada; sedimentology

- and paleogeography of a muddy tidal flat deposit. *Journal of Sedimentary Petrology* 49, 869–889.
- Rolle, J. 2014: *Early Triassic Echinoids of The Western United States: Their Implications for Paleocology and the Habitable Zone Hypothesis following the Permo-Triassic Mass Extinction*. Unpublished PhD thesis, University of Wisconsin Milwaukee.
- Schubert, J.K. & Bottjer, D.J. 1992: Early Triassic stromatolites as post-mass extinction disaster forms. *Geology* 20, 883–886.
- Schubert, J.K. & Bottjer, D.J. 1995: Aftermath of the Permian-Triassic mass extinction event: paleoecology of Lower Triassic carbonates in the Western USA. *Palaeogeography, Palaeoclimatology, Palaeoecology* 116, 1–39.
- Shorb, W.M. 1983: *Stratigraphy, Facies Analysis and Depositional Environments of the Moenkopi Formation (Lower Triassic), Washington County, Utah, and Clark and Lincoln counties, Nevada*. Unpublished Master's Thesis, Duke University, Durham, 205 pp.
- Song, H., Tong, J., Algeo, T.J., Song, H., Qui, H., Zhu, Y., Tian, L., Bates, S., Lyons, T.W., Luo, G. & Kump, L.R. 2014: Early Triassic seawater sulfate drawdown. *Geochimica et Cosmochimica Acta* 128, 95–113.
- Sperling, E.A. & Ingle, J.C. 2006: A Permian-Triassic boundary section at Quinn River Crossing, northwestern Nevada, and implications for the cause of the Early Triassic chert gap on the western Pangean margin. *GSA Bulletin* 118, 733–746.
- Stewart, J.H., Poole, F.G. & Wilson, R.F. 1972: *Stratigraphy and origin of the Triassic Moenkopi Formation and related strata in the Colorado Plateau region*. US Geological Survey Professional Paper 691, 195.
- Sun, Y., Joachimski, M.M., Wignall, P.B., Yan, H., Chen, Y., Jiang, H., Xang, L. & Lai, X. 2012: Lethally hot temperatures during the Early Triassic. *Science* 338, 366–370.
- Twitchett, R. T., Feinberg, J. M., O'Connor, D. D., Alvarez, W., & McCollum, L. B. 2005: Early Triassic Ophiuroids: Their Paleocology, Taphonomy, and Distribution. *PALAIOS* 20(3), 213–223. <https://doi.org/10.2110/palo.2004.p04-30>
- Yochelson, E.L. 1999: Molluscs: overview. In Singer, R. (ed): *Encyclopedia of Paleontology, Volume 2: M–Z*, 754–761. Fitzroy Dearborn Publishers, Chicago.
- Zhu, Q., Aller, R.C. & Fan, Y. 2006: Two-dimensional pH distributions and dynamics in bioturbated marine sediments. *Geochimica et Cosmochimica Acta* 70, 4933–4949.

Supporting Information

Additional supporting information may be found online in the Supporting Information section at the end of the article.

Table S1. All size measurements of SEM images of fossils used in the construction of Figure 5.